Underlining the complexity of the structural and chemical characteristics of ectopic calcifications in breast tissues through FE-SEM and μFTIR spectroscopy

Aicha Ben Lakhdar, Michel Daudon, Marie-Christine Mathieu, Alex Kellum, Corinne Balleyguier, Dominique Bazin

Underlining the complexity of the structural and chemical characteristics of ectopic calcifications in breast tissues through FE-SEM and µFTIR spectroscopy

Aicha Ben Lakhdar[a], Michel Daudon[b,c,d], Marie-Christine Mathieu[a], Alex Kellum[e], Corinne Balleyguier[a], Dominique Bazin[f,g],

[a] Gustave Roussy Institute, service d'anapathologie, 114 Rue Édouard Vaillant, 94805 Villejuif ,France
[b] Sorbonne Universités, UPMC Univ Paris 06, UMR S 702, Paris, France,
[c] INSERM, UMR S 702, Paris, France,
[d] AP-HP, Hôpital Tenon, Explorations Fonctionnelles Multidisciplinaires, Paris, France,
[e] Clemson University, Chemistry department, Clemson, South Carolina
[f] CNRS, LCMCP-UPMC, Collège de France, 11 Place M. Berthelot 75231 Paris Cedex 05, France
[g] Laboratoire de Physique des Solides, Université Paris Sud, Orsay, France

Corresponding author :
Dr. Aicha Ben Lakhdar, Aicha.Benlakhdar@gustaveroussy.fr
Gustave Roussy, service d'anapathologie, 114 Rue Édouard Vaillant, 94805 Villejuif

Abstract : Breast calcifications defined as calcium deposits within breast tissue, can arise from a vast number of aetiologies. Diffuse or scattered distribution is typically seen in benign entities. At the opposite, approximately 95% of all Ductal carcinoma-in-situ, which represents 25-30% of all reported breast cancers are diagnosed because of mammographically detected microcalcifications. In this investigation dedicated to breast calcifications, we assessed at the micrometer scale their chemical nature through last generation microFourier transform Infrared microspectroscopy and their structural characteristics through last generation field emission scanning electron microscopy. Several striking results have been obtained. Heavily mineralized deposits seem to be the results of the agglomeration of micrometer scale spherules. For the first time, we show that these spherules display very different internal structure. Moreover, while Ca phosphate apatite and calcium oxalate dihydrate are the two chemical phases usually reported, we underline the presence of a third chemical phase namely amorphous carbonated calcium phosphate. In the case of duct carcinoma in situ (DCIS), the chemical composition as well as the carbonate level are very inhomogeneous even inside micrometer scale breast calcifications. Moreover, for some samples related to DCIS, special features at the micrometer scale seem to be specific to this pathology.

Keywords : breast cancer, calcifications, micro Fourier Transform Infrared spectroscopy, Field emission scanning electron microscopy,

1. Introduction

Breast cancer is the most common cancer in Europe for females [1], and the most common cancer overall, with more than 464,000 new cases diagnosed in 2012 (29% of female cases and 13% of the total). Breast cancer begins in breast tissue, which is made of glands for milk production, called lobules, and the ducts that connect the lobules to the nipple [2]. Some breast cancers are called *in situ* because they are confined within the ducts (ductal carcinoma in situ or DCIS) or lobules (lobular carcinoma in situ or LCIS) where they originated.

Mammographic mammary microcalcifications are routinely used for the early detection of breast cancer, however the mechanisms by which they form remain unclear [3] and for a long period of time they have been considered as a passive phenomenon [4]. Recently, observations of cell phenotype led M. Scimeca et al. [5] to hypothesize that under specific stimuli, mammary cells may acquire some mesenchymal characteristics transforming themselves into cells with an osteoblast-like phenotype and are able to contribute to the production of breast microcalcifications. At this point, we may recall that the presence of calcification may induce a significant modification of the cellular metabolism, an inflammation or a modification of the phenotype [6,7].

Breast calcifications defined as calcium deposits within breast tissue have thus been at the core of numerous publications [8-25]. One of the difficulties comes from the fact that breast calcifications can arise from a vast number of aetiologies. For example, diffuse or scattered distribution is typically seen in benign entities. At the opposite, approximately 95% of all DCIS, which represents 25-30% of all reported breast cancers are diagnosed because of mammographically detected microcalcifications.

As underlined by T. Oyama et al. [26], two types of calcification have been described. Type I μcalcifications appear as colorless, birefringent crystals composed of weddellite or calcium oxalate dihydrate (CaC_2O_4-$2H_2O$). They most often form in apocrine cysts and less commonly in other benign conditions. Type II μcalcifications, which consist of apatite and occur in both benign and malignant conditions [27,28]. Note that, Calcium oxalate has three different crystalline forms: calcium oxalate monohydrate (whewellite - CaC_2O_4-H_2O) [29-35], is the most stable [36], Calcium oxalate dihydrate [37-40] and finally calcium oxalate trihydrate (caoxite - CaC_2O_4-$3H_2O$) which is rarely observed under physiological conditions [41]. From a chemical point of view, the fact that only calcium oxalate dehydrate is present, a species which normally leads to calcium oxalate monohydrate, seems to indicate that a particular stabilization process exists.

Regarding breast calcifications made of carbonated calcium phosphate apatite (CA), S.H. Poggi *et al.* [42] have described through Scanning Electron Microscopy (SEM) two morphologies, namely spherical entities and heavily mineralized deposits. These authors have also pointed out local composition variations. Finally, R. Baker *et al.* [43] have noticed that the carbonate content of breast CA μcalcifications was shown to be significantly different between benign and malignant disease. The importance of morphology and chemical nature has been underlined for other kinds of pathological calcifications such kidney [31,32,44,45] or prostatic [46,47] calcifications.

Finally, let’s note that the majority of microcalcifications are concretions of varying size composed of calcium phosphates largely in the form of Ca phosphate apatite. In ductal carcinoma in situ, calcifications are formed by deposition of calcium on nuclear debris or in secreted mucosubstances. The other type of microcalcifications, calcium oxalate crystals, is seen in microcysts, especially with apocrine epithelium. This association suggests that

apocrine epithelium is able to synthetize or concentrate and secrete oxalic acid or calcium oxalate.

All these investigations demonstrate clearly that the establishment of a significant relationship between breast μcalcifications and its aetiology calls for a precise structural and chemical description of these biological entities [48,49]. In this study, we have selected a set of breast biopsies in which the presence of apatite calcifications have been already underlined through HES (Hematein-Eosin-Safran) staining procedures performed at the hospital. In order to describe their structural characteristics at the micrometer scale, observations with a Field Emission SEM (FE-SEM) have been done. On the very same samples, their chemical identification at the micrometer scale has been made through μFourier Transform Infra-Red (μFT-IR) spectroscopy [50-56]. Such precise description of these pathological calcifications may lead to a better understanding of their pathogenesis.

2. Experimental

A set of five breast biopsies (Samples A to E) were investigated in order to shed light on the complexity of the structural and chemical characteristics of ectopic calcifications in breast tissues (Table 1). The second set of samples (Samples H to Q) is used to establish a possible relationship between the pathology and the structural and chemical parameters of breast calcifications. In a first step we select benign calcifications and one related to DCIS. The biological samples came from Gustave Roussy Institute (Villejuif, France). Five micrometer sections of biopsies fixed in formalin and paraffin embedded were deposited on low-e microscope slides (MirrIR, Kevley Technologies, Tienta Sciences, Indianapolis). Ethical approval was obtained by the ethical committee of IGR for this study. Each sample was only named by a study number, without indication of the name of the patient or potential identification data.

Table 1 : Physiological and clinical data of the first set of samples

Sample	Age (years)	Disease
Sample A – 13H2480	65	Normal breast (duct)
Sample B - 13H2606	60	Fibroadenoma
Sample C – 13H2282	61	Galactophoric cyst
Sample D - 13H2427	57	Adenosis
Sample E -13H2281	62	Ductal carcinoma in situ (DCIS)

Table 2 : Physiological and clinical data of the second set of samples

Sample	Age (years)	Disease
Sample F - 13H3279	60	DCIS
Sample G - 13H6529	55	DCIS
Sample H - 13H2851	66	DCIS
Sample I - 13H1096	70	DCIS
Sample J - 13H8746	66	DCIS
Sample K - 14H2554	37	Benign
Sample L - 14H4540	50	Benign
Sample M - 13H4111	63	Benign

A Zeiss SUPRA55-VP SEM was used for observation of microstructure. This field-effect "gun" microscope (FE-SEM) operates at 0.5-30 kV. High-resolution observations were obtained by two secondary electron detectors: an in-lens SE detector and an Everhart-Thornley SE detector. To maintain the integrity of the samples, measurements were performed at low voltage (between 0.5 and 2 kV) without the usual deposits of carbon at the surface of the sample [57,58].

IR microspectroscopy was performed on an IN10MX microscope (Thermo Scientific) for recording large maps. All spectra were collected in ultrafast mode using a 50 µm × 50 µm aperture. The spectra were collected in the 4000 - 700 cm^{-1} mid-IR range at a resolution of 8 cm^{-1} with one spectrum per pixel. Data analysis of IR spectra and chemical images was performed using OMNIC software (Thermo Scientific). Infrared spectroscopy was also carried out on a PerkinElmer Spotlight 400 FTIR microspectrometer fitted with a liquid nitrogen cooled, 16-element linear array mercury cadmium telluride (MCT) detector. All FTIR spectra were collected in the mid-infrared from 4000 cm^{-1} to 650 cm^{-1} using 16 cm^{-1} spectral resolution and 64 accumulations for each collection by the array.

3. Results and discussion

From a crystallographic point of view, the apatite prototype structure was first determined by Naray-Szabo [59] and are conventionally regarded as conforming to $A_5(BO_4)_3X$ general chemical formula ($P6_3/m$ symmetry) [60]. At this point we would like to recall that hydroxyapatite can be described as a hexagonal stacking of $(PO_4)^{3-}$ groups with two kinds of tunnel parallel to the c axis. The first one coincides with the ternary axis of the structure and is occupied by Ca^{2+}, noted as Ca(I) ions. The second one is linked by oxygen and other calcium ions, noted Ca(II), and is occupied by OH^- ions. Ca(I) and Ca(II) are present in a 2/3 ratio [61-63].

Regarding biological samples, CA calcifications display generally a hierarchical structure at different scales [64-66]. Biological apatites result from an agglomeration of nanocrystals [67,68]. Their nanometer size with an anisotropy along the c axis [69] is combined with a high Ca and OH^- deficiency [70,71]. CO_3^{2-} carbonate groups [72] and trace elements [73] such as Mg^{2+} [74-76], Zn^{2+} [77-83] or Sr^{2+} [84-87] can be found inside or at their surface while an amorphous part (ACCP for amorphous carbonated calcium phosphate) [88] is located at the surface of the nanometer size crystal. CO_3^{2-} carbonate anions substitute partially phosphate ions (PO_4^{3-}) (B-type) or hydroxide ions (OH^-) (A-type). For the position of CO_3^{2-} ions (A-type) six possibilities around the c-axis are in fact possible for a same chemical composition [89]. Interestingly, a supplementary species of carbonate, i.e. a labile carbonate has been underlined [90]. Thus biological apatites can be represented by the following formulae :

$Ca_{10-x+u}\square_{x-u}(PO_4)_{6-x}(CO_3)_x(OH)_{2-x+2u}$ with $\square$ corresponding to vacancy, $x \leq 2$ and $u \leq x/2$).

At the micrometre scale, different morphologies can be observed for CA calcifications. In a recent paper focused on kidney stones [91], CA particles appeared as spherules of 4.5 ± 3.0 µm in diameter and were significantly larger in females than in males. Note that spherical entities have been also identified in human cardiovascular tissue calcification [92]. Also, the description of the surface of CA particles may provide major clinical information regarding infection process involved in CA formation as shown for kidney stones [93].

Investigations performed through vibrational spectroscopies, namely µFTIR and Raman spectroscopies, have been also used for studying biological CA [94-100]. Raman experiments

may also play a major role regarding the guidance of stereotactic breast needle biopsies for microcalcifications [101]. I. Barman et al. [102] show the potential of Raman spectroscopy to concomitantly detect microcalcifications and diagnose associated lesions. Such investigation provides real-time feedback to radiologists during such biopsy procedures, reducing non-diagnostic and false-negative biopsies. Quite recently, it was found from Raman spectroscopic analysis of CA μcalcifications that carbonate content is greater in CA calcifications from benign breast tissue than in malignant breast tissue [103]. Also, a significant correlation was observed between carbonate concentrations and carcinoma in-situ sub-grades [14]. Taking into account the small size of the crystallites, Raman spectroscopy seems to be even more effective than FTIR but this technique has several drawbacks. Some patients present extremely low quantities of ectopic calcification with fragile, organic, micrometer-sized crystals; we have already observed that chemical characterization through Raman spectroscopy even at very low power induces significant alterations of their morphology. Moreover, even in the case of ectopic calcifications made of whewellite microcrystals, Raman spectroscopy can induce significant modifications. As a preliminary conclusion, all these studies underline the different structural parameters which have to be discussed in the case of CA calcifications [104].

The starting point of this study is given by FE-SEM observations performed on benign calcifications (sample A-13H2480). On figure 1, a set of FE-SEM photographs at low and high magnifications has been gathered. As we can see, normal breast calcifications can be observed in detail.

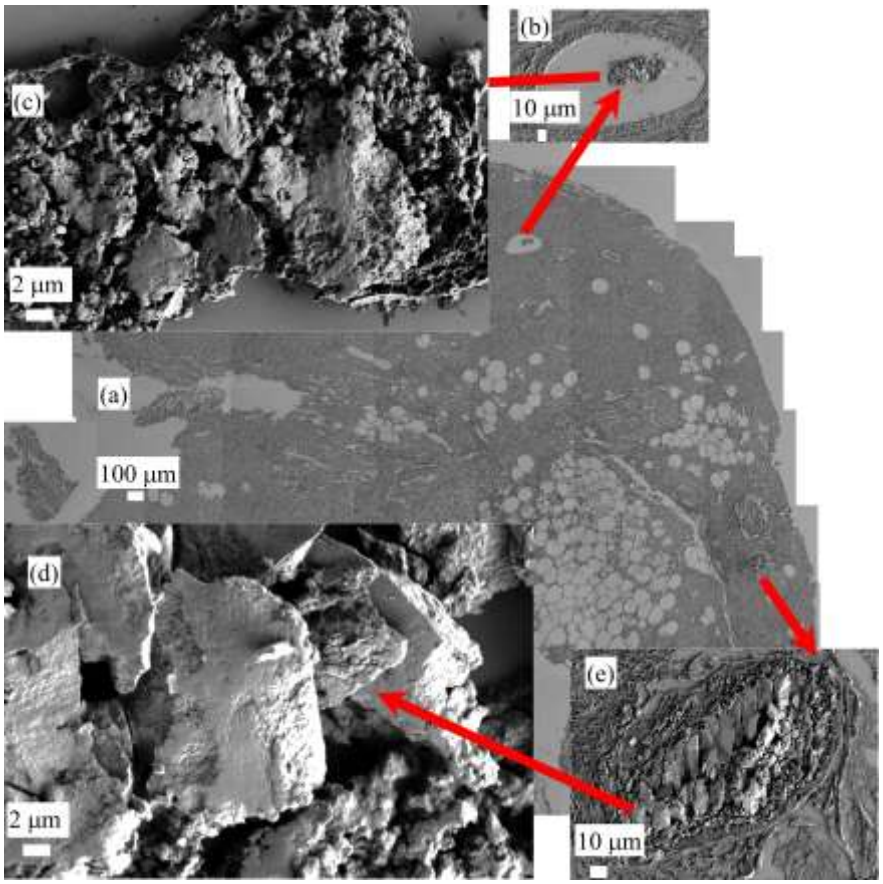

Fig. 1. FE-SEM observations of sample A (13H2480 - Normal breast) at low (a) and high (b,c,d,e) magnifications. Different mineralized deposits at various magnifications can be visualized.

On figure 2, we have considered the sample B (13H2606) (which is related to fibroadenoma. In that case, heavily mineralized deposits (black arrows on figure 2a) as well as micrometer scale spherules at different magnifications (inside black circle on figure 2a) and then on figures 2b and 2c at higher magnifications) are shown.

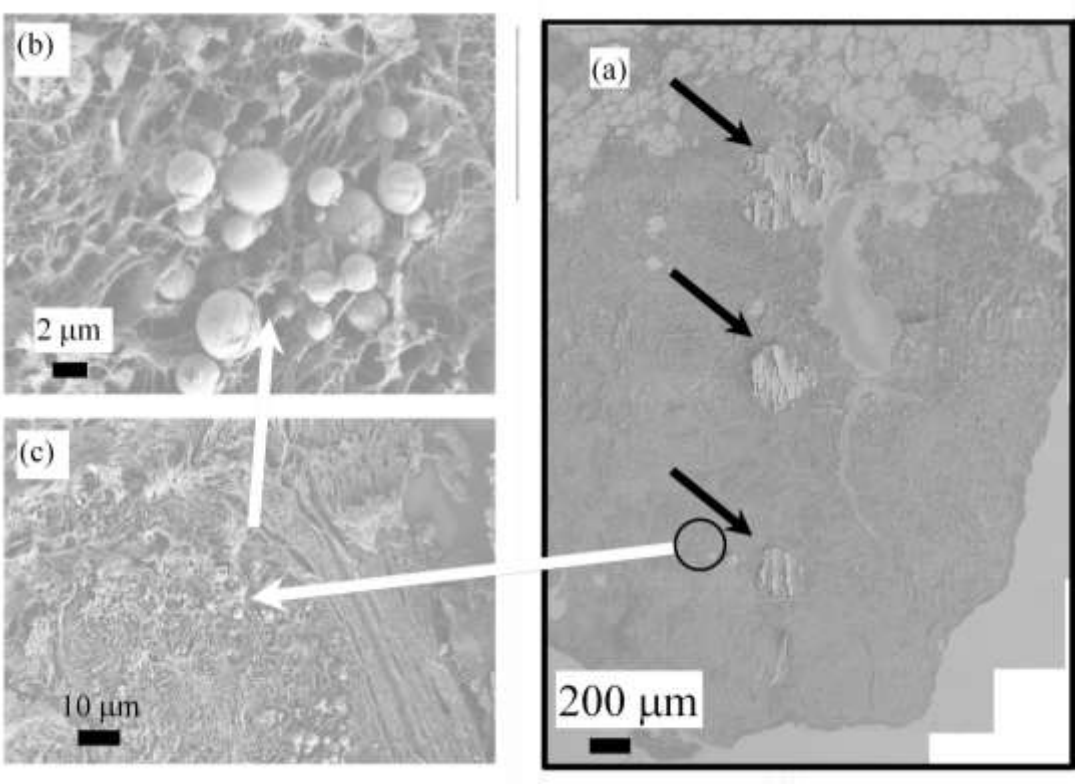

Fig. 2. (a) FE-SEM observations of sample B (13H2606- Fibroadenoma) showing heavily mineralized deposits and very small entities invisible at this magnification. (b) and (c) micrometer scale spherules corresponding to the black circle of Fig 2(a) are visualized at higher magnifications.

Such observation is in line with previous measurements performed by S.H. Poggi et al. [42] which have already underlined the presence of two kinds of CA deposits. More interesting, another set of SEM observations establish a possible link between these two kinds of CA deposits. As we can see on fig. 3a to 3h, heavily mineralized deposits seem to be the results of the agglomeration of micrometer scale spherules. Such structural evolution from micrometer scale spherules to “large” deposits is observed for very different pathologies including fibroadenoma (sample B), galactophoric cyst (sample C) and adenosis (sample D).

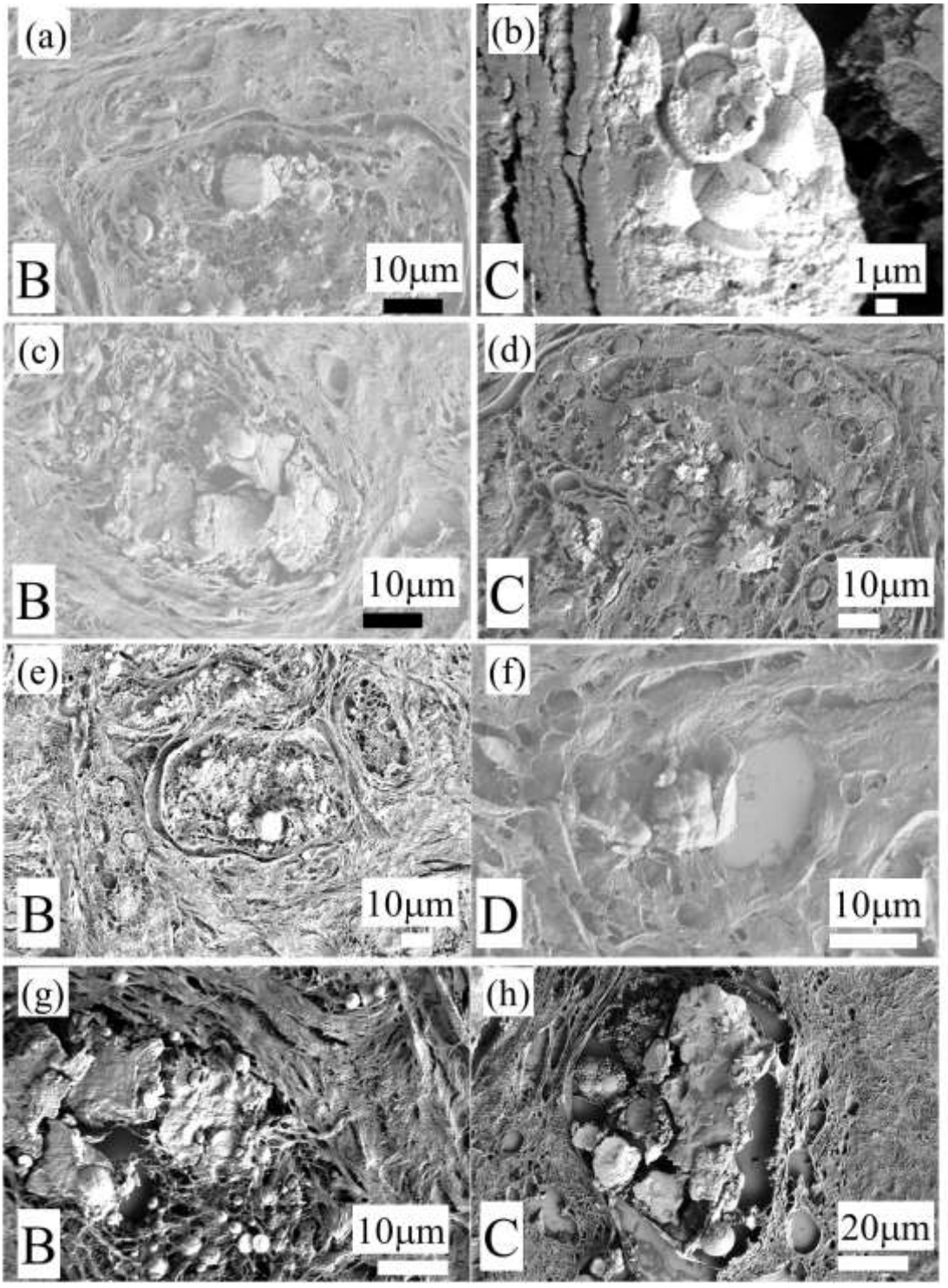

Fig. 3. (a-h) All these SEM observations (Sample B: 13H2606- Fibroadenoma ; Sample C : 13H2282 Galactophoric cyst ; Sample D : 13H2427 - Adenosis) show that some of heavily mineralized deposits seems to be the result of the agglomeration of micrometre scale spherules.

Thanks to the development of the FE-SEM technology, it is possible now to get a more precise description of these spherules. The following set of SEM observations which have been collected on the same sample (sample B) demonstrates clearly that spherical entities may display very different internal structure (Fig. 4). Some of them are homogeneous (Fig. 4a) while for others, concentric layers are present at the surface of the spherules (Fig. 4b and 4c). Finally, some spherules seem to exhibit a radial structure (Fig. 4a and 4d).

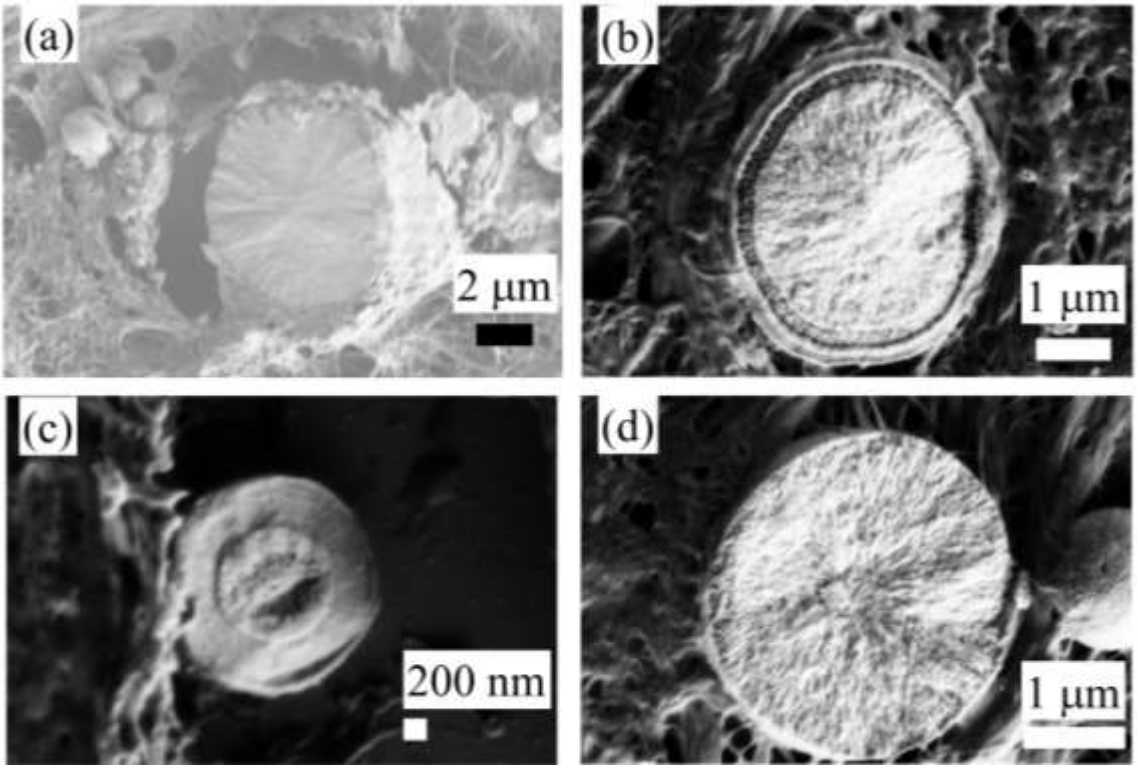

Fig. 4. Sample B (13H2606- Fibroadenoma). Different internal structure for CA sphericules. (a) Radial structure; (b) and (c) Concentric layers are present at the surface of homogeneous structure; (d) Radial structure.

In order to determine precisely the chemical nature of these abnormal deposits, FTIR experiments have been performed (Fig. 5 for the sample E, Fig. 6 for the sample C (13H2282- Galactophoric cyst). As we can see on figures 5 and 6, last generation FTIR experimental device allows the acquisition of large map in a short time (around 30 mn) with an excellent signal to noise ratio. Let's just recall that FTIR spectroscopy probes the vibrational modes of molecules, providing a spectrum that is structure specific [105].

On figure 5 (Sample E - 13H2281 – Ductal carcinoma in situ), data collected on the FTIR experimental set up and on the FE-SEM device have been gathered. Fig. 5a shows the optical map obtained while on figure 5c a typical infrared spectrum is shown. The absorption bands measured at 960-962 cm^{-1} and 1035-1045 cm^{-1}, correspond to ν_1 and ν_3 P-O stretching vibrations respectively, while the ν_4 O-P-O bending mode corresponds to the doublet at 602-563 cm^{-1} (figure 5b). The absorption band corresponding to the ν_3 P-O 1030-1045 cm^{-1} is clearly visible while the doublets appearing at around 1410 cm^{-1} and 1450 cm^{-1} are due to the presence of carbonate inside the CA crystals. The spatial repartition of CA (figure 5c) can be estimated through a plot of the spatial repartition of the intensity of the absorption peak located at 1030 cm^{-1} (ν_3 P-O). In the case of sample 1, this spatial repartition of CA (figure

7c) given with FTIR data is in line with the SEM map (Fig. 7d). Thus, we have for this breast biopsy a chemical imaging as well as the morphology of the different CA deposit.

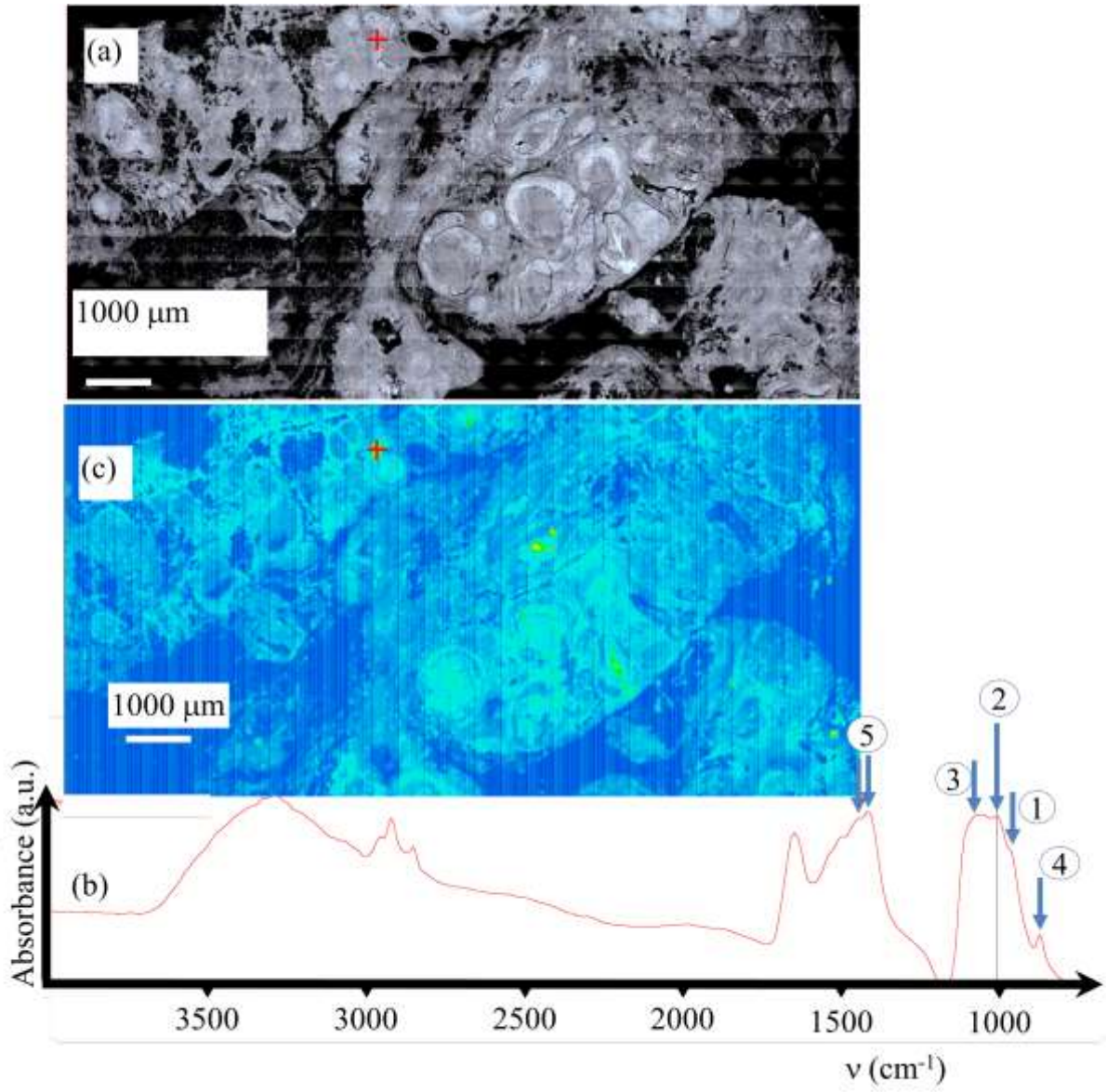

Fig. 5. Sample E (13H2281 – Ductal carcinoma in situ) (a) Optical image collected by the FTIR spectrometer. (b) Typical infrared spectrum: (1) ν_1 P-O stretching vibration modes are measured at 960-962 cm^{-1}; (2) ν_3 P-O stretching vibration modes are measured at 1035-1045 cm^{-1}; (3) Particular attention has to be paid to the presence of a feature in the ν_3 absorption band, which can be used as a fingerprint for the presence of ACCP; (4,5) absorption bands due to the presence of carbonate. (c) Spatial repartition of Ca phosphate apatite in the breast biopsy. Red cross on figures 5a and 5c corresponds to the point of measurement.

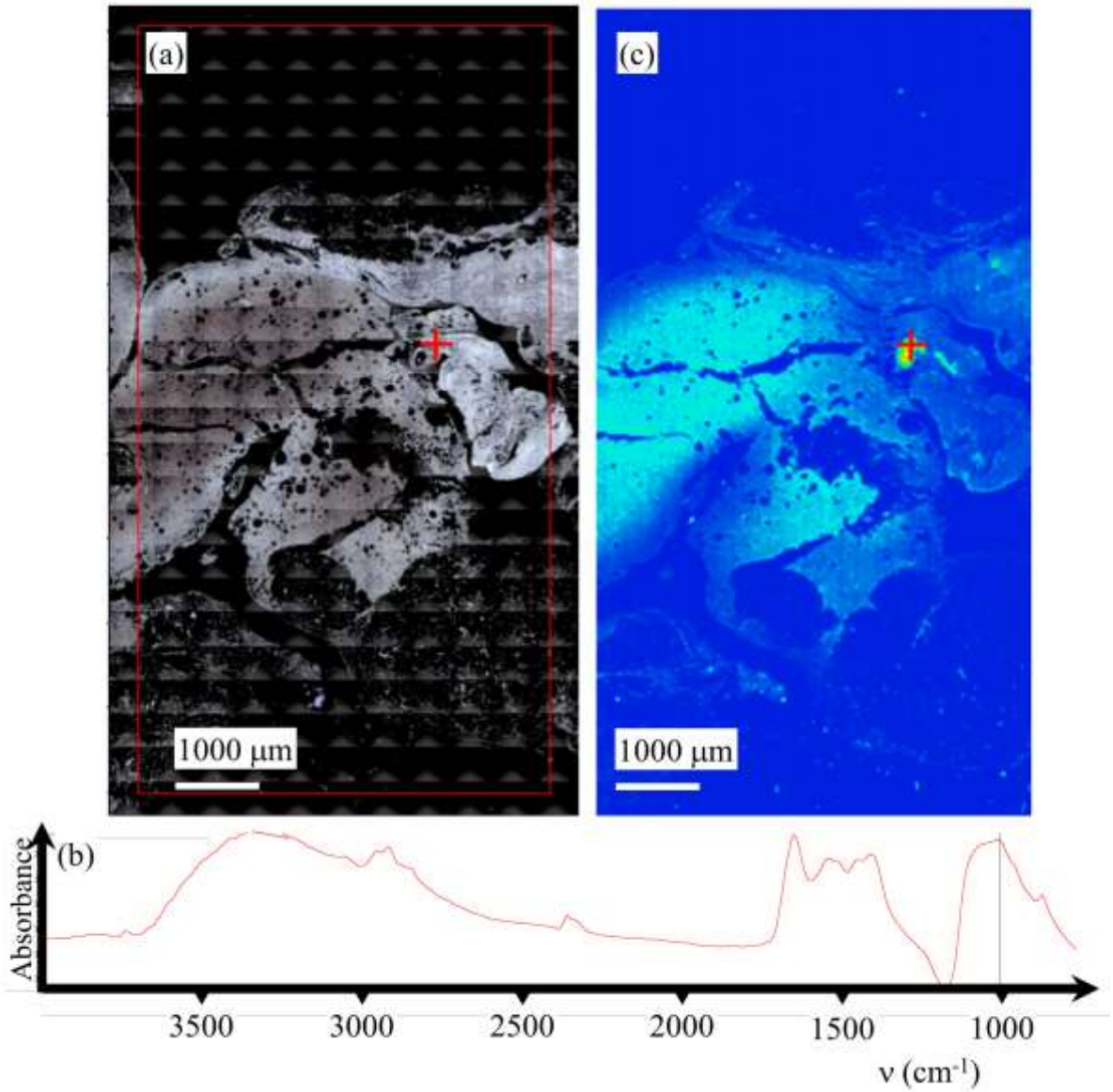

Fig. 6. Sample C (13H2282- Galactophoric cyst) (a) Optical image collected by the FTIR spectrometer. (b) Typical infrared spectrum. (c) Spatial repartition of Ca phosphate apatite in the breast biopsy as given by the absorption bands at 1000 cm^{-1}. Red cross on figures 6a and 6c corresponds to the point of measurement.

Particular attention has to be paid to the presence of a shoulder in the ν_3 absorption band, which can be used as a fingerprint for the presence of amorphous carbonated calcium phosphate (ACCP). Its disappearance can be considered as a marker for the presence of ACCP compound, the ν_3 P-O peak of which being shifted at around 1060 cm^{-1}. For the three samples (F, C and G) which correspond respectively to ductal carcinoma in situ, galactophoric cyst and sclerosis adenosis, FT-IR spectroscopy underlines the presence of ACCP. To our knowledge, such chemical phase has never been identified in breast calcification.

Finally, we would like to discuss the sample E (13H2281-Ductal carcinoma in situ, for which we compare different FTIR spectra collected for a same calcification. On figures 7, SEM images of this structure which correspond to duct carcinoma in situ at two different magnifications are shown (Fig. 7a and 7b). Note that it was not possible to visualize spherical entities.

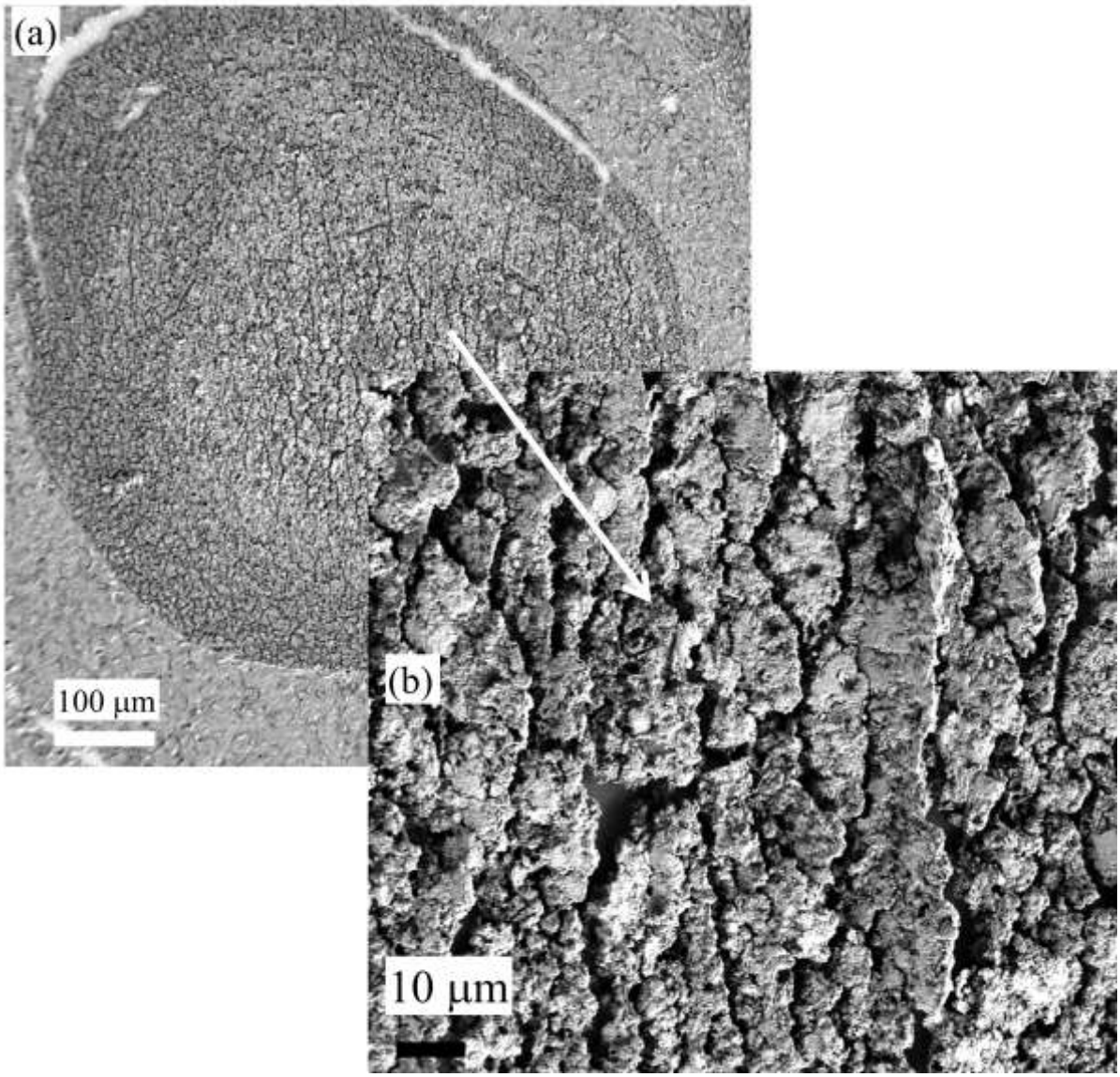

Fig. 7. Sample E (13H2281-Ductal carcinoma in situ) : (a) and (b) SEM observations at two different magnifications. Note the absence of spherical entities.

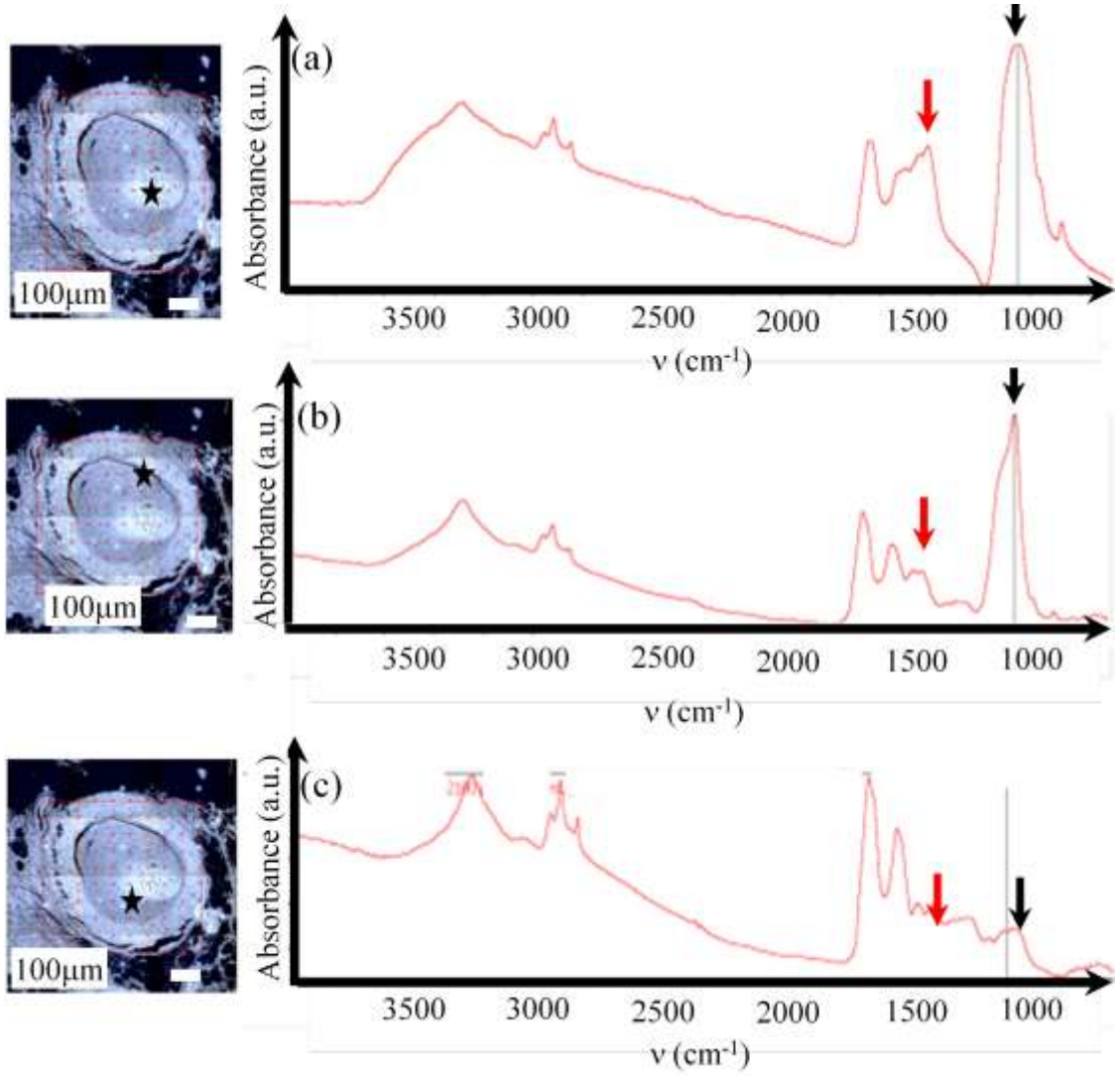

Fig. 8. Sample E (13H2281-Ductal carcinoma in situ) (a, b and c) Location (given by the black star on the optical photography) and FTIR spectra. The chemical composition as well as the carbonate level are very inhomogeneous: a) high proportion of PACC (black arrow) with a very high carbonation rate (red arrow); b) high proportion of CA (black arrow) with a low carbonation rate (red arrow); c) spectrum of proteins with a low proportion of calcium phosphate (black arrow).

Then, for this feature, we collect FTIR spectra from the core to the surface (Fig. 8a, b and c). It is crystal clear that these three spectra show clearly a significant chemical heterogeneity inside the calcification. As underlined previously, the presence of a shoulder in the ν_3 absorption band is directly related to the presence of CA and its disappearance to ACCP and a comparison between the two IR spectra plotted on fig. 8a and 8b is significantly different. Moreover, for this feature, a major variation of the CO_3^{2-}/PO_4^{3-} ratio is observed.

We would like to assess now the second set of samples (Samples F to M) for which we try to establish a possible relationship between the physicochemical characteristics of the calcifications and the pathology. On these samples, μFTIR experiments as well as FE-SEM observations at different magnifications have been performed. As an illustration, experiments on sample F (Figures 9 and 10) and sample K (Figures 11 and 12) are shown. For both samples, μFTIR data indicate the presence of ACCP and CA.

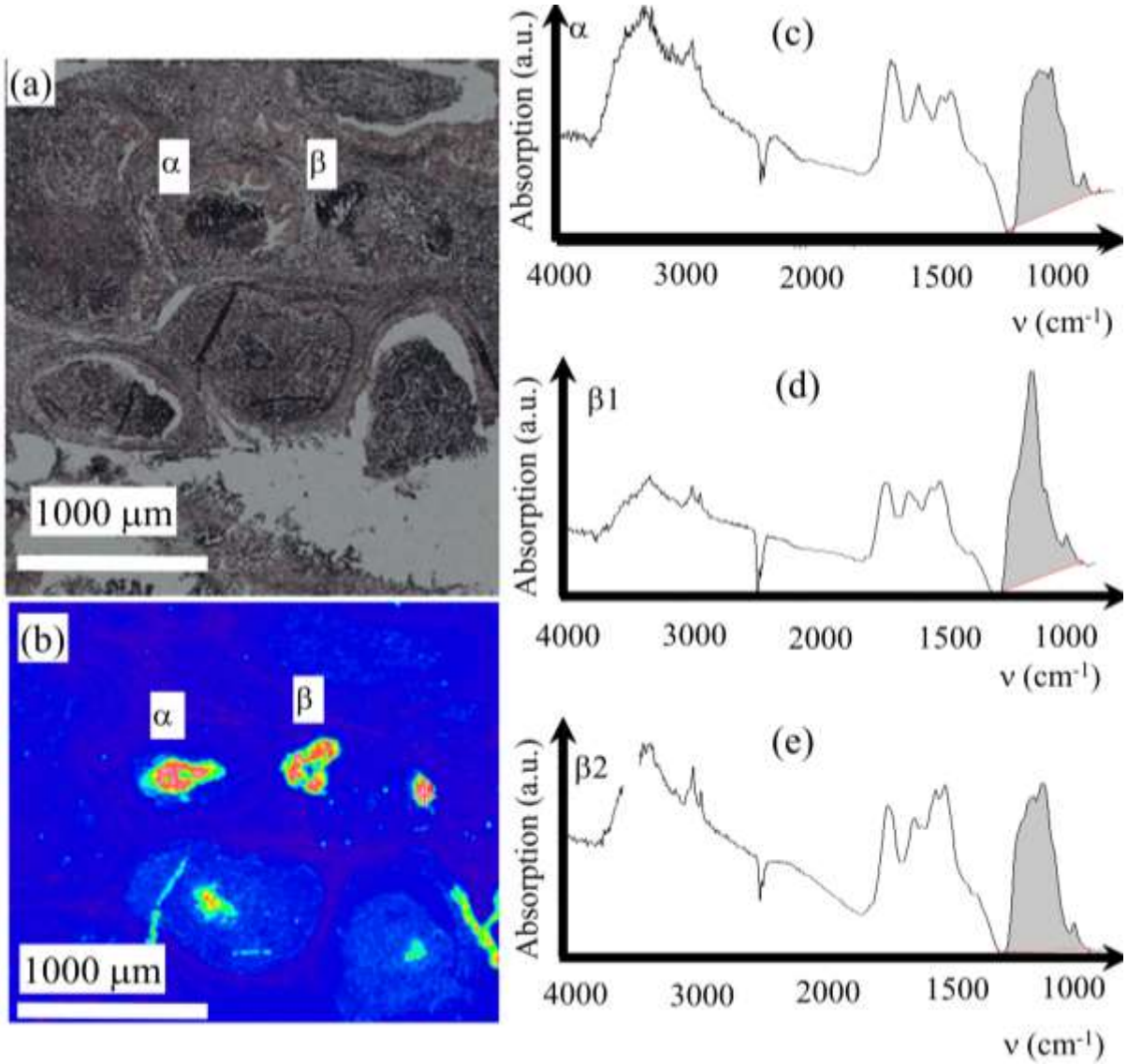

Fig. 9. Sample F - 13H3279 - DCIS: (a) Optical image collected by the FTIR spectrometer. (b) Spatial repartition of Ca phosphate apatite in the breast biopsy as given by the absorption bands at 1000 cm^{-1}. (c) infrared absorption spectrum collected for the deposit α.(d) and (e) two infrared absorption spectra collected for the deposit β showing various mixing of ACCP and CA.

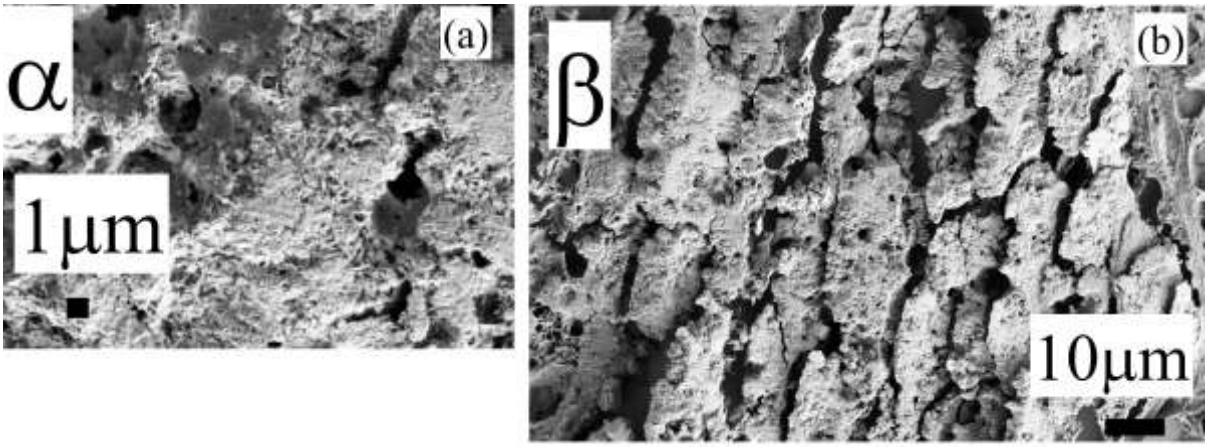

Fig. 10. Sample F - 13H3279 –DCIS : (a) and (b) SEM observations at high magnification for the deposits α and β.

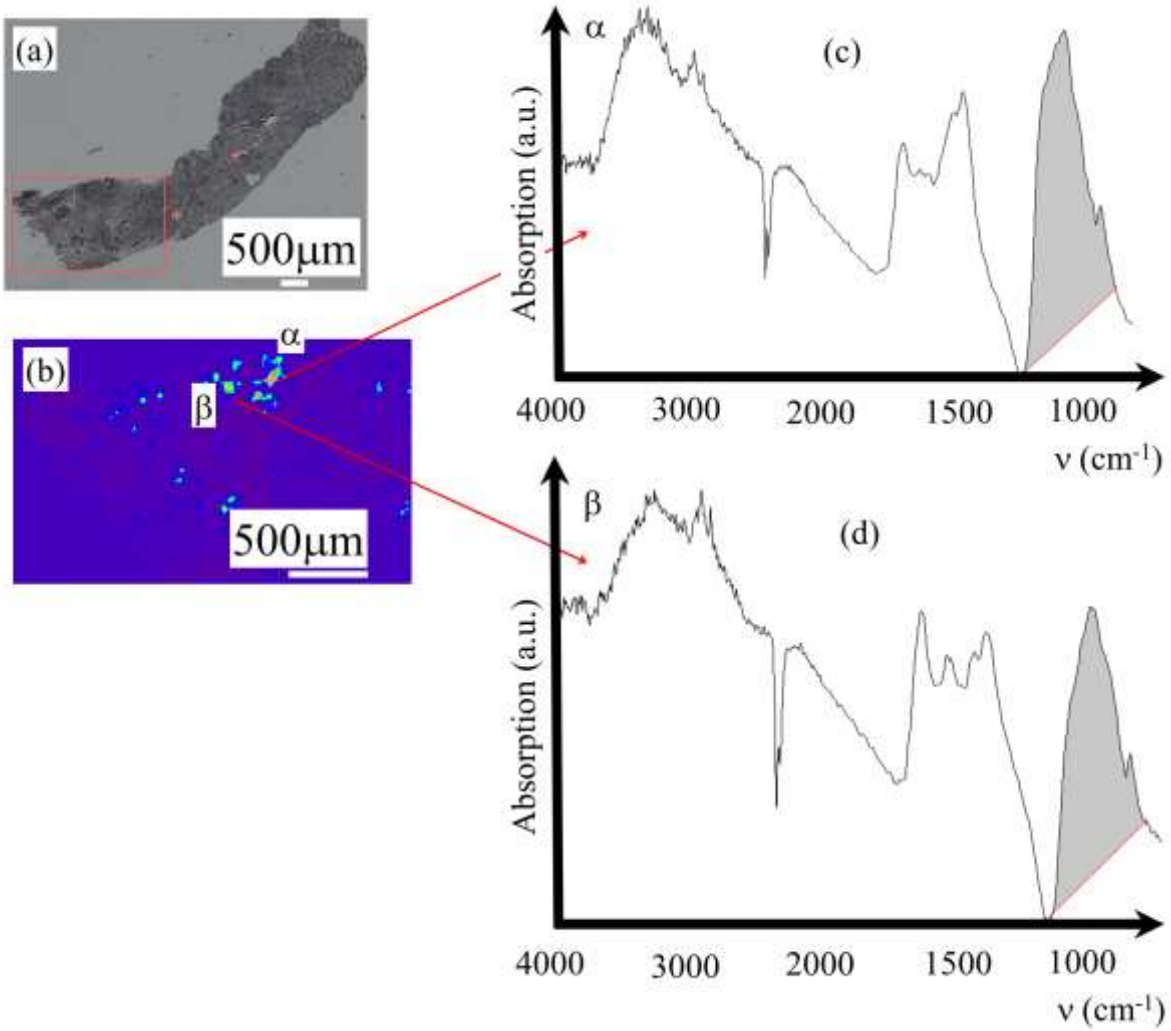

Fig. 11. Sample K - 14H2554- benign : (a) Optical image collected by the FTIR spectrometer. (b) Spatial repartition of Ca phosphate apatite in the breast biopsy as given by the absorption bands at 1000 cm^{-1}. (c) and (d) Infrared absorption spectrum collected for the deposit α and β.

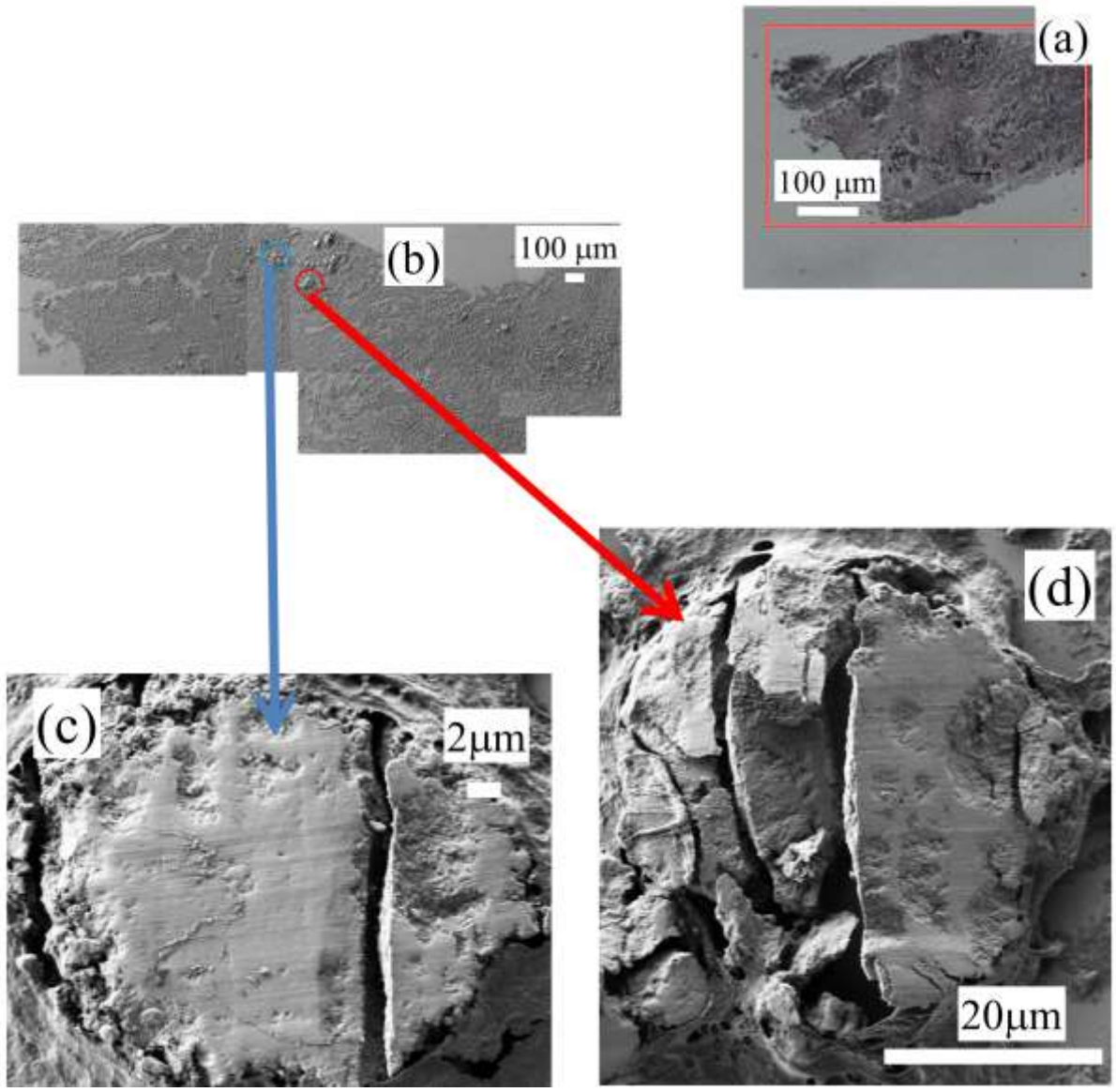

Fig. 12. Sample K - 14H2554- benign: (a) optical map, FE-SEM observations at low (b) and high (c,d) magnifications.

At a first sight, the complete set of observations performed through FE-SEM seems to show that the two kinds of calcifications are quite similar (Fig. 13) One striking point is related to the fact that for some samples (samples E,F and G) related to DCIS, FE-SEM observations clearly show a specific morphology at the micrometer scale (fig. 14).

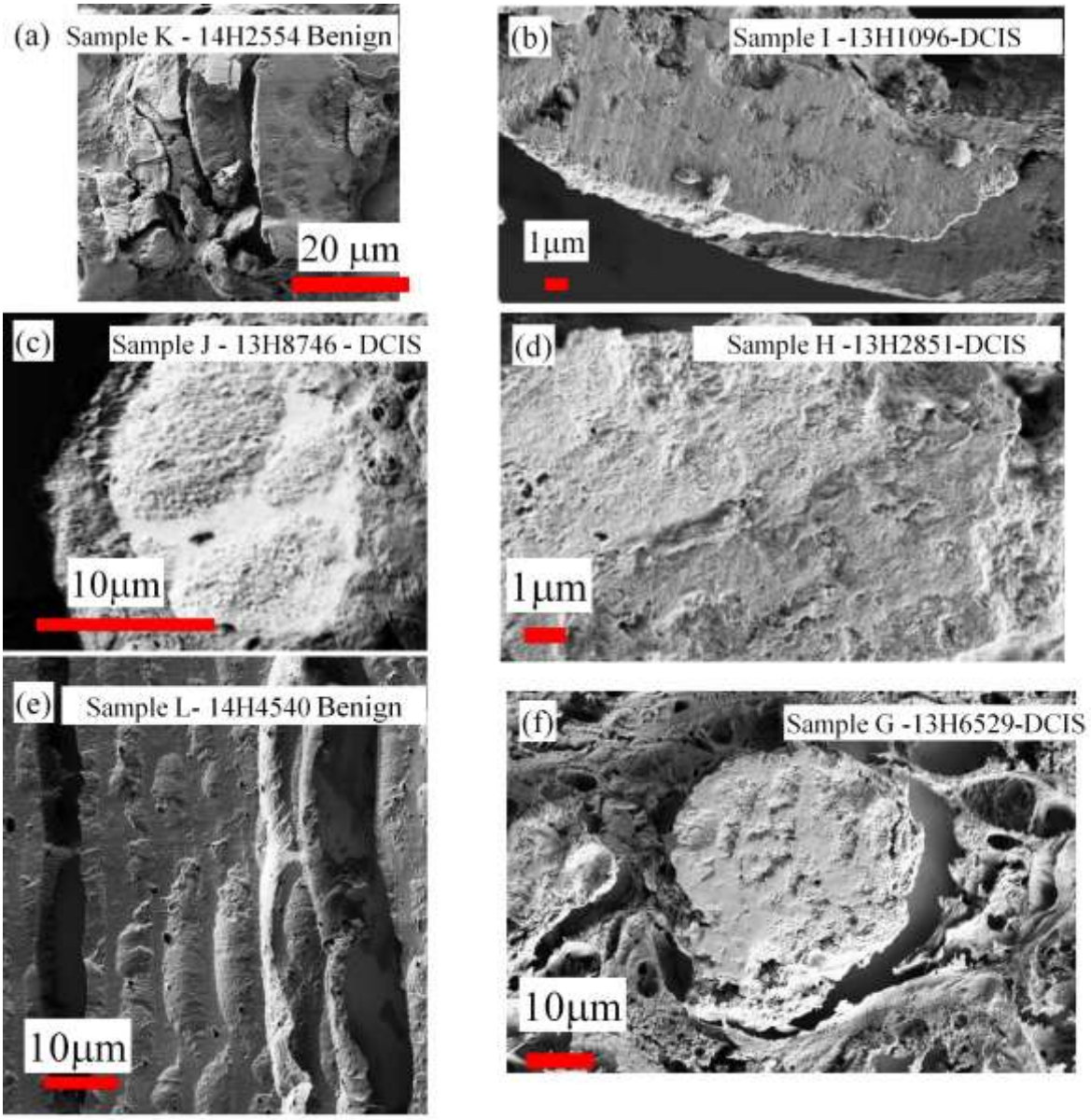

Fig. 13.SEM observations collected for different samples. Samples K and L are related to benign calcifications while samples G,H and I are related to DCIS.

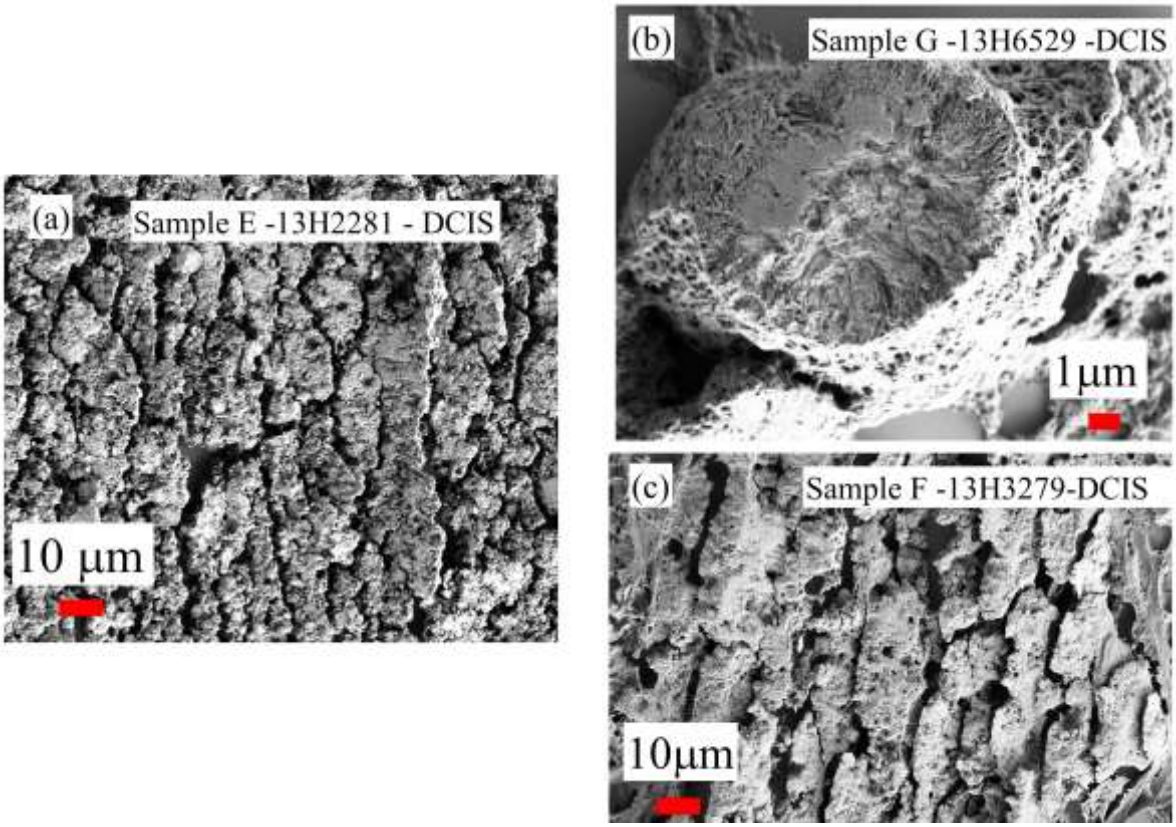

Fig. 14. SEM observations collected for breast calcifications (samples E,F and G) related to DCIS.

4. Conclusion

In this investigation, we have characterized ectopic calcifications in breast tissues using last generation experimental devices i.e. FE-SEM and µFTIR spectrometer. Such approach allows us to describe the morphology of these mineral deposits and to identify precisely their chemical nature. Several striking results have been obtained. While the literature regarding ectopic calcifications in breast tissues [see for example 8-25, 106-110] shows that only two chemical phases have been identified, through a careful analysis of µFTIR spectroscopy, our study demonstrates clearly the presence of a third phase, namely ACCP (fig8, sample E). In the case of duct carcinoma in situ, this chemical phase was present at the centre of the duct. At our best knowledge, it is the first time that this chemical phase has been reported in ectopic calcifications. Through µFTIR spectroscopy, we underline a very inhomogeneous distribution of the chemical phases as well as the carbonate levels in the pathological calcifications. It is thus very difficult to relate the carbonation rate of CA to the pathology as previously suggested. Finally, SEM observations underline a diversity in the internal structure of spherule entities. For some samples related to DCIS, special features at the micrometer scale seem to be related to this pathology because they were not found for the other pathologies. In order to establish a relationship between the physicochemical characteristics of the calcifications and pathology, a double blind trial has to be performed.

Moreover, as underlined in previous publications, we can add data coming from other techniques. In the case of ectopic calcifications made of apatite, the presence of trace elements such Zn which can play a major role in the pathogenesis, has to be assessed through X-ray fluorescence [111-122] and one technique specific to synchrotron radiation, namely X-ray absorption spectroscopy (XAS) [123-130]. For example, it is possible to underline inflammation process through the content of Zn, an information which can be very important

for the clinician [115,116]. Through XAS, it is also possible to assess the localisation of trace elements versus the calcification [130].

Disclosure
All the authors declared no competing interests.

Acknowledgments
This work was supported by the Physics and Chemistry Institutes of CNRS and by contracts ANR-09-BLAN-0120-02, ANR-12-BS08-0022, ANR-13-JSV-10010-01, convergence UPMC CVG1205 and CORDDIM-2013-COD130042. Thanks to different experiments performed on ectopic calcifications using the Soleil SR Facility (proposal numbers DISCO-20130967, SMIS- 20130016, DISCO-20120747, SMIS-20120070, SMIS-20110084, SMIS-20100566, DISCO- 20100565, DISCO-20100505, DISCO-20100502, SMIS-20100039, DIFFABS-20060357, DIFFABS-20080028, DIFFABS-20110059) which allow us to start this research.

References

[1] http://www.cancerresearchuk.org
[2] American Cancer Society. Breast Cancer Facts & Figures 2011-2012. Atlanta: American Cancer Society, Inc.
[3] R. F. Cox, M. P. Morgan, Bone 53 (2013) 437.
[4] G.C. Busin, U. Keppler,V. Menges, Virchows Arch A Pathol Anat Histopathol 393 (1981) 303–307.
[5] M. Scimeca, E. Giannini, C. Antonacci, C.A. Pistolese, L.G. Spagnoli, E. Bonanno, BMC Cancer 14 (2014) 286.
[6] C.M. Giachelli, Z Kardiol. 90 (2001)31.
[7] D. Bazin, J.-Ph. Haymann, E. Letavernier, J. Rode, M. Daudon, Presse Med. 43 (2014) 135.
[8] O. Anastassiades, V. Bouropoulou, G. Kontogeorgos, M. Rachmanides, Pathology Research Practice 178 (1984) 237.
[9] L. Frappart, M. Boudeulle, J. Boumendil, H.C. Lin, I. Martinon, C. Palayer Y. Mallet-Guy, D. Raudrant, A. Bremond, Y. Rochet, Human Pathology 15 (1984) 880.
[10] T.C. Holme, M.M. Reis, A. Thompson, A. Robertson, D. Parham, P. Hickman, P.E. Preece, Eur Surg Oncol 19 (1993) 250.
[11] R. Tang, J. Liu, W. Gao, Chinese J. of Cancer Research 10 (1998)215.
[12] F. Schmidt, E. Sorantin, C. Szepesvari, E. Graif, M. Becker, H. Mayer, K. Hartwagner, Phys. Med. Biol. 44 (1999) 1231.
[13] M. Castellanos, S. Varma, K. Ahern, S.-J. Grosso, S. Buchbinder, D. D'Angelo, C. Raia, M. Kleiner, S. Elsayegh, Am. J. of Kidney Diseases 48(2006)301.
[14] R. Baker, P. Matousek, K. L. Ronayne, A. W. Parker, K. Rogers, N. Stone, Analyst 132 (2007) 48.
[15] G. M. Tse, P.-H. Tan ,H.S. Cheung,W. C. W. Chu,W.W. M. Lam, Breast Cancer Res Treat 110 (2008) 1.
[16] C. Kendall, M. Isabelle, F. Bazant-Hegemark, J. Hutchings, L. Orr, J. Babrah, R. Baker, N. Stone, Analyst 134 (2009) 1029.
[17] R. Gallagher, G. Schafer, M. Redick, M. Inciradi, W. Smith, F. Fan, O. Tawfik, Annals of Diagnostic Pathology 16 (2012) 196.
[18] D. Bazin, M. Daudon, Ch. Combes, Ch. Rey, Chem. Rev. 112 (2012) 5092.
[19] D. Bazin, M. Daudon, J. Phys. D: Appl. Phys. 45 (2012) 383001.
[20] T.-C. Hsiao, Y.-Y. Cheng, W.-T. Tein, S.-B. Luo, D.-Y. Chiou, R.-J. Chung, M.-L. Li J. of Biomedical Optics 18(2013)66002.
[21] H. Ling, Z.-B. Liu, L.-H. Xu, X.-L. Xu, G.-Y. Liu, Z.-M. Shao, Asia-Pacific J. of Clinical Oncology 9 (2013) 139.
[22] L. Holmberg, Y N S Wong, L. Tabár, A. Ringberg, P. Karlsson, L.-G. Arnesson, K. Sandelin, H. Anderson, H. Garmo, S. Emdin British J. of Cancer 108 (2013) 812.
[23] J.-J. Li, C. Chen, Y. Gu, G. Di, J. Wu, G. Liu, Z. Shao, PLoS ONE 9 (2014) e88853.
[24] J.-Y. Han, J. Lee, E.-K. Kim, S. Shin, M. Kang, K.-C. Lee, K. Nam, J. of Medical Ultrasonics 41 (2014) 39.
[25] H. Mohamed, M.S. Mabrouk, A. Sharawy Computer Methods and Programs in Biomedicine 116 (2014) 226.
[26] T. Oyama, T. Sano, T. Hikino, Q. Xue, K. Iijima, T. Nakajima, F. Koerner, Virchows Arch. 440 (2002) 267.
[27] L.D. Truong, J. Cartwright, L. Alpert, Mod. Pathol. 5 (1992) 146.

[28] C. Tornos, E. Silva, A. El-Naggar, K.P. Pritzker
Am. J. Surg. Pathol.14 (1990) 961.
[29] V.Tazzoli, C. Domeneghetti, Am. Mineral. 65 (1980) 327.
[30] T. Echigo, M. Kimata, A. Kyono, M. Shimizu, T. Hatta, Mineral. Mag. 69 (2005) 77.
[31] M. Daudon, D. Bazin, G. André, P. Jungers, A. Cousson, P. Chevallier, E. Véron
G. Matzen, J. Appl. Cryst. 42 (2009) 109.
[32] M. Daudon, P. Jungers, D. Bazin, New Engl. J. Med. 359 (2008) 100.
[33] H. Colas, L. Bonhomme-Coury, C. Coelho Diogo, F. Tielens, F. Babonneau,
Ch. Gervais, D. Bazin, D. Laurencin, M.E. Smith, J.V. Hanna, M. Daudon,
Ch. Bonhomme, Cryst. Eng. Comm. 15 (2013) 8840.
[34] A. Millan, Crystal Growth & Design 1(2001) 245.
[35] T. Fei, X. Hao, S. Bao-Lian, Analytical Methods 5 (2013) 6900.
[36] A.R. Izatulina, Y.O. Punin, A.G. Shtukenberg, O.V. Frank-Kamenetskaya,
V.V. Gurzhiy, Minerals as Advanced Materials II 2012, 415.
[37] C. Sterling, Acta Cryst. 18 (1965) 917.
[38] P. Brown, D. Ackermann, B. Finlayson, J. of Crystal Growth 98 (1989) 285.
[39] A. V. Rusakov, O. V. Frank-Kamenetskaya, V. V. Gurzhiy, M. S. Zelenskaya,
A. R. Izatulina, K. V. Sazanova, Crystallography Reports 59 (2014) 362.
[40] C. Conti, M. Casati, C. Colombo, M. Realini, L. Brambilla, G. Zerbi,
Spectrochimica Acta Part A: Molecular and Biomolecular Spectroscopy, 128(2014)413.
[41] R.C. Walton, J. P. Kavanagh, B. R. Heywood, P.N. Rao,
J. Cryst. Growth, 284 (2005) 517.
[42] H. Poggi, H.C.W. Skinner, J. J. Ague, D. Carter, Am. Mineralogist 83 (1998) 1122.
[43] R. Baker, K.D. Rogers, N. Shepherd, N. Stone, British J. of Cancer 103 (2010) 1034.
[44] A. Dessombz, E. Letavernier, J.-Ph. Haymann, D. Bazin, M. Daudon
The J. of Urology, In Press.
[45] M. Daudon, D. Bazin, E. Letavernier, Urolithiasis 43 (2015) 5.
[46] A. Dessombz, P. Méria, D. Bazin, E. Foy, S. Rouzière, R. Weil, M. Daudon
Progrès en urologie 21(2011) 940.
[47] A. Dessombz, P. Méria, D. Bazin, M. Daudon, PLoS ONE 7(2012)e51691.
[48] D. Bazin, M. Daudon, P. Chevallier, S. Rouzière, E. Elkaim, D. Thiaudière, B. Fayard,
E. Foy, P.A. Albouy, G. André, G. Matzen, E. Véron, Ann. Biol. Clin. 64 (2006) 125.
[49] M. Daudon, D. Bazin, J. Phys.: Conference Series 425 (2013) 022006.
[50] N. Quy-Dao, M. Daudon M (1997) Infrared and Raman Spectra of Calculi.
Elsevier.
[51] E.V. Wilson, M.J. Bushiri, V.K. Vaidyan,
Spectrochimica Acta Part A 77(2010)442.
[52] A. Dessombz, D. Bazin, P. Dumas, Ch. Sandt, J. Sule-Suso,
M. Daudon, PLoS ONE 6 (2011) e28007.
[53] I. Faklaris, N. Bouropoulos, N. A. Vainos, Crystal Research and Technology
48 (2013)632.
[54] S. Gràcia-Garcia, F. Millán-Rodríguez, F. Rousaud-Barón, R. Montañés-Bermúdez,
O. Angerri-Feu, F. Sánchez-Martín, H. Villavicencio-Mavrich, A. Oliver-Samper
Actas Urológicas Españolas 35(2011)354.
[55] M. Pucetaite, S. Tamosaityte, A. Engdahl, J. Ceponkus, V. Sablinskas, P. Uvdal,
Central European J. of Chemistry 12 (2014) 44.
[56] F. Blanco, P. Ortiz-Alías, M. López-Mesas, M. Valiente
J. of Biophotonics, in press.
[57] Brisset F, Repoux M, Ruste J, Grillon F, Robaut F., Microscopie électronique à
balayage et Microanalyses, EDP Sciences, 2009. ISBN : 978-2-7598-0082-7.

[58] D. Bazin, M. Daudon, Annales de Biologie Clinique, sous presse.
[59] S. Naray-Szabo Z. Kristallogr Kristallgeom Kristallphys Kristallchem 75 (1930) 387.
[60] T.J. White, D. Zhi Li Acta Cryst. B 59 (2003) 1.
[61] R. W. G. Wyckoff, (1965). Crystal Structures, Vol. 3, Inorganic Compounds Rx(MX4)y, Rx(MnXp)y, Hydrates and Ammoniates, pp. 228-234. Ed. New York: John Wiley and Sons.
[62] D. McConnell (1973). Apatite, Its Crystal Chemistry, Mineralogy, Utilization, and Geologic and Biologic Occurrences. Ed. Wein : Springer-Verlag.
[63] S. Cazalbou, D. Eichert, X. Ranz, C. Drouet, Ch. Combes, M.F. Harmand, Ch. Rey J. Mater. Sci. Mater. Med. 16 (2005) 405.
[64] J.D. Currey, Science 309 (2005) 253.
[65] S. Mann, Nature 365 (1993) 499.
[66] J.C. Elliott JC (1994) Structure and chemistry of the apatites and other calcium orthophosphates. Elsevier, Amsterdam
[67] M.I. Kay, R.A. Young, A.S. Posner, Nature 204 (1964) 1050.
[68] D. Bazin, C. Chappard, C. Combes, X. Carpentier, S. Rouzière, G. André G. Matzen, M. Allix, D. Thiaudière, S. Reguer, P. Jungers, M. Daudon, Osteoporos Int. 20 (2009) 1065.
[69] M. Vallet-Regi, J.M. Gonzales Calbet, Prog Solid State Chem 32 (2004) 1.
[70] Ch. Rey, J.L. Miquel, L. Facchini, A.P. Legrand, M.J. Glimcher, Bone 16 (1995) 586.
[71] G. Cho, Y. Wu, J.L. Ackerman, Science 300 (2003) 1123.
[72] G. Penel, G. Leroy, Ch. Rey, E. Bres, Calcif Tissue Int 63 (1998) 475.
[73] T. Tamm, M. Peld, J. Solid State Chem. 179 (2006) 1581.
[74] I. Mayer, J.D.B. Featherstone, R. Nagler, M. Noejovich, D. Deutsch, I. Gedalia J. of Solid State Chemistry 56 (1985) 230.
[75] L. Müller, E. Conforto, D. Caillard, F.A. Müller, Biomolecular Engineering 24 (2007) 462.
[76] A. Farzadi, F. Bakhshi, M. Solati-Hashjin, M. Asadi-Eydivand, N. Azuan abu Osman Ceramics Internat. 40 (2014) 6021.
[77] D. Bazin, X. Carpentier, O. Traxer, D. Thiaudière, A. Somogyi, S. Reguer, G. Waychunas, P. Jungers, M. Daudon, J. Synchrotron Rad. 15 (2008) 506.
[78] D. Bazin, X. Carpentier, I. Brocheriou, P. Dorfmuller, S. Aubert, Ch. Chappard, Biochimie 91 (2009) 1294.
[79] Y. Tang, H.F. Chappell, M.T. Dove, R.J. Reeder, Y.J. Lee, Biomaterials 30 (2009) 2864.
[80] S. Gomes, J.M. Nedelec, E. Jallot, D. Sheptyakov, G. Renaudin, Chem. of Mat. 23(2011) 3072.
[81] S. Gomes, J.M. Nedelec, G. Renaudin, Acta Biomaterialia, 8 (2012)1180.
[82] R.F.B. Resende, G.V.O. Fernandes, S.R.A. Santos, A.M. Rossi, I. Lima, J.M. Granjeiro, M.D. Calasans-Maia, J. of Mat. Science – Mat. in med. 24 (2013) 1455.
[83] S. Gomes, A. Kaur, J.M. Nedelec, G. Renaudin, J. of Mat. Chem. B 2 (2014) 536.
[84] A. Bigi, E. Boanini, C. Capuccini, M. Gazzano, Inorg. Chim. Acta 360 (2007) 1009.
[85] D. Bazin, M. Daudon, Ch. Chappard, J. J. Rehr, D. Thiaudière, S. Reguer J. Synchrotron Rad. 18 (2011) 912.
[86] C.G. Frankr, A.C. Raffalt, K. Stahl, Calcified Tissue Internat. 94 (2014) 248.
[87] D. Bazin, A. Dessombz, Ch. Nguyen, H. K. Ea, F. Lioté, J. Rehr, Ch. Chappard, S. Rouzière, D. Thiaudière, S. Reguer, M. Daudon, J. Synchrotron Rad. 21 (2014) 136.
[88] S. Cazalbou, D. Eichert, C. Drouet, C. Combes, C. Rey,

C. R. Palevol. 3 (2004) 563.
[89] Y. Suetsugu, Y. Takahashi, F.P. Okamura, J. Tanaka,
J. Solid State Chem 155 (2000) 292.
[90] C. Rey, B. Collins, T. Goehl, R.I. Dickson, M.J. Glimcher,
Calcif. Tissue Int. 45(1989) 157.
[91] X. Carpentier, M. Daudon, O. Traxer, P. Jungers, A. Mazouyes, G. Matzen, E. Véron,
D. Bazin, Urology 73 (2009) 968.
[92] S. Bertazzo, E. Gentleman, K.L. Cloyd, A.H. Chester, M. H. Yacoub, M. M. Stevens,
Nat. Mater. 12 (2013) 576.
[93] D. Bazin, G. André, R. Weil, G. Matzen, E. Véron,
M. Daudon, Urology 79 (2012) 786.
[94] N. Pleshko, A. Boskey, R. Mendelsohn, J. Biophys 60 (1991) 786.
[95] R. Manoharan, K. Shafer, L. Perelman, J. Wu, K. Chen, G. Deinum, M. Fitzmaurice
J. Myles, J. Crowe, R.R. Dasari, M.S. Feld,
Photochem. Photobiol. 67 (1998) 15.
[96] K. E. Shafer-Peltier, A.S. Haka, M. Fitzmaurice, J. Crowe, J. Myles, R.R. Dasari
M.S. Feld, J. Raman Spectrosc. 33(2002) 552.
[97] H.J. Gulley-Stahl, S. B. Bledsoe, A.P. Evan, A.J. Sommer,
App. Spectroscopy 64 (2010) 15.
[98] A. Dessombz, P. Méria, D. Bazin, M. Daudon, PLoS One 7 (2012) e51691.
[99] N. Stone, R. Baker, K. Rogers,A.W. Parker, P. Matousek
Analyst 132 (2007) 899.
[100] N. Stone, P. Matousek, Cancer Res. 68 (2008) 4424.
[101] A. Saha,I. Barman, N.C. Dingari, L.H. Galindo,A. Sattar, W. Liu, D. Plecha, N. Klein,
R.R. Dasari, M. Fitzmaurice, Anal. Chem. 84(2012)6715.
[102] I. Barman, N.C. Dingari, A. Saha, S. McGee, L.H. Galindo, W. Liu, D. Plecha,
N. Klein, R.R. Dasari, M. Fitzmaurice, Cancer Res. 73(2013)3206.
[103] A.S. Haka, K.E. Shafer-Peltier, M. Fitzmaurice, J. Crowe, R.R. Dasari, M.S.Feld,
Cancer Res. 62 (2002) 5375.
[104] D. Bazin, J.-Ph. Haymann, E. Letavernier, J. Rode, M. Daudon,
Presse Med. 43 (2014) 135.
[105] L.M. Miller, P. Dumas, Curr Opin Struct Biol. 20 (2010) 649.
[106] P. Henrot, A. Leroux, C. Barlier, P. Génin
Diagnostic and Interventional Imaging 95 (2014)141.
[107] C.C. Diaz-Huerta, E.M. Felipe-Riveron, L.M. Montaño-Zetina
Expert Systems with Applications 41 (2014) 7361.
[108] M. Sakakibara, J. Yokomizo, N. Shiina, T. Kazama, R. Nakamura, H. Fujimoto,
T. Nagashima, H. Takishima, Y. Nakatani, M. Miyazaki,
J. of the American College of Surgeons 219 (2014) 295.
[109] P. Machado, J.R. Eisenbrey, B. Cavanaugh, F. Forsberg
Ultrasound in Medicine & Biology, In Press.
[110] R. Scott, C. Kendall, N. Stone, K. Rogers
Anal. Methods 6 (2014) 3962.
[111] J. Susini, M. Salomé, B. Fayard, R. Ortega, Surf. Rev. Lett. 09(2002) 203.
[112] M. Lankosz, M. Szczerbowska-Boruchowska, J. Chwiej, J. Ostachowicz,
A. Simionovici, S. Bohic, Spectrochimica Acta Part B: 59(2004)1517.
[113] D. Bazin, P. Chevallier, G. Matzen, P. Jungers, M. Daudon
Urol. Res. 35 (2007)179.
[114] E. Kosior, S. Bohic, H. Suhonen, R. Ortega, G. Devès, A. Carmona, F. Marchi,
J.-F. Guillet, P. Cloetens, J. of Structural Biology 177(2012)239.

[115] S. Bohic, M. Cotte, M. Salomé, B. Fayard, M. Kuehbacher, P. Cloetens, G. Martinez-Criado, R. Tucoulou, J. Susini, J. of Structural Biology 177(2012)248.
[116] A. Dessombz, Ch. Nguyen, H.-K. Ea, S. Rouzière, E. Foy, D. Hannouche, S. Réguer, F.-E. Picca, D. Thiaudière, F. Lioté, M. Daudon, D. Bazin, J. of Trace Elements in Medicine and Biology 27 (2013) 326.
[117] X. Carpentier, D. Bazin, Ch. Combes, A. Mazouyes, S. Rouzière, P.A. Albouy E. Foy, M. Daudon, J. of Trace Elements in Medicine and Biology 25 (2011) 160.
[118] J. Kuta, J. Machat, D. Benova, R. Cervenka, J. Zeman, P. Martinec, Env. Geom. and Health 35 (2013) 511.
[119] V.K. Singh, P.K. Rai, Biophysical Reviews 6 (2014) 291.
[120] M. West, A.T. Ellis, Ph.J. Potts, Ch. Streli, Ch. Vanhoof, P. Wobrauschek, J. Anal. At. Spectrom. 29 (2014) 1516.
[121] L. Louvet, D. Bazin, J. Büchel, S. Steppan, J. Passlick-Deetjen, Z.A. Massy PLoS ONE 10 (2015) e0115342.
[122] B. Hannache, A. Boutefnouchet, D. Bazin, M. Daudon, E. Foy, S. Rouzière, A. Dahdouh, Progrès en Urologie 25 (2015) 22.
[123] D.E. Sayers, F.W. Lytle, E.A. Stern, Adv. X-ray Anal. 13 (1970) 248.
[124] D. C. Bazin, D. A. Sayers, J. J. Rehr, J. Phys. Chem. B 101 (1997) 11040.
[125] D. Bazin, C.R. Chimie 17 (2014) 615.
[126] D. Eichert, M. Salomé, M. Banu, J. Susini, C. Rey Spectrochimica Acta Part B: Atomic Spectroscopy 60(2005)850.
[127] D. Bazin, M. Daudon, C. Chappard, J.J. Rehr, D. Thiaudière, S. Reguer, J. Synchrotron Rad. 18(2011)912.
[128] Ch. Nguyen, H.K. Ea, D. Thiaudiere, S. Reguer, D. Hannouche, M. Daudon, F. Lioté, D. Bazin, J. Synchrotron Rad. 18 (2011)475.
[129] G. Veronesi, E. Koudouna, M. Cotte, F.L. Martin, A.J. Quantock, Anal. Bioanal. Chem. 405(2013)6613.
[130] Ch.G. Frankær, A.Ch. Raffalt, K. Stahl, Calcif Tissue Int 94(2014)248.
[131] T. Sugiyama, M. Uo, T. Wada, D. Omagari, K. Komiyama, T. Noguchi, Y. Jinbu, M. Kusam, BioMetals 28 (2015)11.